Published in final edited form as:
Circ Heart Fail. 2008 September ; 1(3): 192–199. doi:10.1161/CIRCHEARTFAILURE.108.768465.

Titin Isoforms, Extracellular Matrix and Global Chamber Remodeling in Experimental Dilated Cardiomyopathy: Functional Implications and Mechanistic Insights

Wissam A. Jaber, MD, **Calin Maniu, MD**, **Judith Krysiak, MSc**[†], **Brian P. Shapiro, MD**, **Donna M. Meyer**, **Wolfgang A. Linke, PhD**[†], and **Margaret M. Redfield, MD**

[†]Mayo Clinic and Foundation, Rochester MN and Physiology and Biophysics Unit, University of Muenster, Schlossplatz 5, D-48149 Muenster, Germany

Abstract

Background—Altered titin isoforms may modify cardiac function in heart failure (HF) but the nature of isoform switches and associated functional implications are not well defined. Limited studies have reported increased compliant isoform (N2BA) expression in human systolic HF. Titin may also modulate stretch-regulated responses such as myocardial natriuretic peptide (NP) production.

Methods and results—We characterized titin isoform expression and extracellular matrix (ECM) in all four cardiac chambers and the LV epi- and endocardium in normal dogs (n=6) and those with HF (n=6) due to tachypacing and characterized functional implications at the LV myofiber and chamber level. Recognizing the potential for uncoupling of the ECM and cardiomyocyte in tachypacing, we also assessed myocardial NP production, a molecular marker of stretch-regulated responses. All chambers were dilated in HF but the ECM was not increased. HF dogs had markedly lower N2BA in atria and right ventricle (RV). In failing LV, N2BA was decreased only in the epicardium where myofiber passive stiffness was increased. However, LV chamber mechanics were driven by the marked LV dilatation with no increase in LV diastolic stiffness. NP levels increased dramatically in the endocardium in relation to increases in LV wall stress.

Conclusion—Tachypacing HF is characterized by decreases in compliant titin isoform expression in the atria, RV and LV epicardium. However, LV chamber mechanics are principally determined by geometric and ECM changes rather than titin-based myofiber stiffness in this model. Stretch-regulated myocardial responses (NP production) appeared intact suggesting that the mechanotransduction role of titin was not impaired in HF.

Keywords

Diastole; Heart Failure; Mechanics; Remodeling

Introduction

Experimental tachycardia related cardiomyopathy (TRCM) is a unique model of dilated cardiomyopathy (DCM) and heart failure (HF). TRCM is associated with marked left ventricular (LV) dilatation, systolic dysfunction and disruption of the fibrillar collagen network

Address for correspondence: Margaret M. Redfield, MD Mayo Clinic and Foundation 200 First Street SW Rochester, MN 55905 Tel: (507) 284-1281; Fax: (507) 266-4170; redfield.margaret@mayo.edu.

Dr's Jaber and Maniu contributed equally to this study.

[1–7]. Further, reduced myocyte adhesion to constituents of the basement membrane [4,8] has been reported in TRCM and may contribute to myocyte elongation, chamber remodeling and dysfunction, as well as altered mechanotransduction due to decreased coupling of the myocyte sarcolemma to the extracellular matrix (ECM).

Titin is a giant sarcomeric protein which exists in the heart in two isoforms co-expressed at the level of the sarcomere: the shorter, stiffer N2B and various longer, more compliant N2BA isoforms. Differential expression of these isoforms is related to alternate gene splicing, influences passive stiffness of the sarcomere and along with geometric changes, hypertrophy and the ECM may contribute to myocardial and chamber mechanics in all cardiac chambers [9,10]. Titinand titin-associated proteins may play a pivotal role in mechanotransduction in the heart by regulating the bi-directional interaction between wall stress, the ECM and the sarcomere [9]. Indeed, defects in Z-disk-based mechanotransduction involving Z-disk-based binding partners of titin are associated with an inability to up-regulate natriuretic peptide (NP) production in response to stretch in vitro [11].

Mechanisms regulating differential titin isoform expression and the role of these isoform changes in influencing cardiac function in disease states are not well defined. Studies of titin isoform changes in chronic human cardiomyopathy, including DCM [12–14], and experimental TRCM [15,16] to date are few and have yielded somewhat counter-intuitive findings. Further, understanding of the influence of titin isoform-mediated changes in sarcomeric stiffness on myofiber and chamber mechanics is complicated by interaction with changes in the quantity or character of the ECM, hypertrophy and altered chamber geometry, variables which may be co-regulated by factors influencing titin-isoform expression.

The objectives of the current study were to characterize titin-isoform expression, hypertrophy and ECM changes in all cardiac chambers and in the LV epi- and endocardium in normal and TRCM canine hearts; to characterize the functional implications of these changes at the LV myofiber and chamber level and to examine the relationship between wall stress, titin isoform changes, and ECM remodeling. Recognizing the putative roles of titin and titin-isoform changes to sense and compensate for increases in ECM-based stiffness [9,12–14] and the potential for uncoupling of the ECM and cardiomyocyte in TRCM, we also determined whether increases in wall stress were associated with increases in NP production, a molecular marker of stretch-regulated responses.

Methods

Study design

The study included 6 young normal (NL) mongrel dogs and 6 dogs with HF due to TRCM. Conscious echocardiography followed by an open-chest hemodynamic study under anesthesia and tissue harvest was performed. All experimental procedures were designed in accordance with NIH guidelines and approved by the Mayo Institutional Animal Care and Use Committee. Dogs were euthanized by intravenous potassium chloride, consistent with guidelines of the Panel on Euthanasia of the American Veterinary Medical Association. The authors have full access to and take full responsibility for the integrity of the data. All authors have read and agree to the manuscript as written.

HF model

Under general anesthesia (ketamine 10 mg/kg, diazepam 0.5 mg/kg and isoflurane 0.5–2.5%), a modified, programmable cardiac pacemaker and a permanent screw-in right ventricular epicardial lead were placed through a left thoracotomy as previously described [6]. After a two week recovery period, the pacemaker was programmed to 180 beats per minute for ten days

after which the pacing rate was increased at seven day intervals sequentially to 200, 210, 220 and 240 beats per minutes as previously described [6,7].

Echocardiography

All dogs underwent 2 D guided m mode echocardiography in the conscious state and with pacing suspended briefly (HF dogs) for measurement of LV internal dimension and wall thickness in systole and diastole and left atrial (LA) area and volume as previously described [17]. Venous blood was drawn for hormone analysis.

Hemodynamic study

In HF dogs, the pacemaker was turned off immediately prior to the hemodynamic study. Animals were anesthetized with fentanyl (0.25 mg/kg bolus then 0.18 mg/kg/hr) and midazolam (0.75 mg/kg bolus then 0.59 mg/kg/hr) and ventilated with supplemental oxygen. The heart was exposed via a sternotomy and stabilized in a pericardial cradle. Animals were instrumented with a high fidelity micromanometer catheter in the LV, short and long axis endocardial piezoelectric crystals, pneumonic inferior and superior vena cava occluders and an atrial pacing wire. Animals were atrial paced at 10 to 20 bpm above sinus rate. Steady state data were obtained. A 500-mL bolus of normal saline was then given to insure that end diastolic pressure volume data during vena cava occlusion would span a range reflecting the entire curvilinear end diastolic pressure volume relationship (EDPVR). Steady-state data before and after volume expansion were collected. Data during vena cava occlusion were collected immediately after volume expansion to define the end-systolic pressure volume relationship (ESPVR) and the EDPVR. Animals were sacrificed and the heart was harvested. The LV, LA, right ventricle (RV) and right atrium (RA) were separated and weighed adding the ventricular and atrial septum to the LV and LA respectively. The LV samples were bisected to provide equal endocardial and epicardial sections. All tissues were flash frozen in liquid nitrogen and stored at −80° centigrade while other sections were immediately placed in formalin and paraffin embedded for staining and histological analysis.

Hemodynamic analysis

Digital data were acquired at 4 ms intervals and analyzed using customized software (Sonometrics; London, Canada). To characterize the EDPVR, end diastolic pressure (EDP) and volume (EDV) points obtained from multiple beats during vena cava occlusion were fit to the monoexponential equation $EDP = \alpha \cdot e^{\beta \cdot EDV}$ where α is the curve-fitting constant and β is the stiffness coefficient using least-squares non-linear regression [18]. To reflect the combined effects of diastolic properties and LV remodeling and to account for the covariance between α and β, a measure of LV capacitance was calculated, EDV_{20} (=Log[20/α]/β), or LV EDV at a theoretical pressure of 20mmHg. β was normalized for wall volume (Vw; $\beta_{Normalized}$= β*Vw) as previously described [18]. The LV midwall stress (σ, at end systole and end diastole) was estimated using the LV pressure, LV cavity volume, and Vw in a spherical model and the dimensionless myocardial stiffness index (κ) was calculated from the EDPVR data as previously described [18]. Similar methods were used to calculate end diastolic LA midwall stress using echo derived LA volume, LA wall volume and LV EDP. The ESPVR was characterized as: end systolic pressure (ESP)=Ees(ESV-V_0) where ESV = end systolic volume and Vo = the x intercept of the extrapolated ESPVR [18].

Tissue analysis

Plasma and LV atrial (ANP) and canine brain (cBNP) NP concentrations were measured by radio-immunoassay as previously described with tissue concentrations normalized to protein concentration measured by the Lowry method [19,20]. Total collagen content in cardiac tissue was quantified using the hydroxyproline assay [21] and indexed to tissue weight. LV and LA

samples were stained with picrosirus red for measurement of collagen volume fraction using quantitative histomorphometry as previously described [21]. All analyses on LV were performed in endo- and epicardial tissues and as the tissue samples were equally bisected, endo- and epicardial values were averaged for overall LV data.

Titin isoform composition and myofiber stiffness

Tissue samples were processed and loaded onto a 2% SDS-polyacrylamide gel to measure relative concentrations of the titin isoforms N2B and N2BA as previously described [13,14]. Mean titin-isoform composition was obtained by averaging densitometry data for at least ten gel lanes per tissue type. Passive tension of isolated, Triton X-100-skinned, myofiber bundles (diameter, 200–300 μm; length, 2.5–3.0 mm) was determined as described [13]. Sarcomere length was measured by laser diffractometry [13]. The means of nine individual fiber measurements on epi- and endocardial samples from two dogs in each group were averaged.

Statistics

Results are presented as mean ± standard deviation. Given the small number of dogs and the large variation, groups were compared using the Wilcoxon Rank Sums non-parametric test, the p-values of which were reported in the Tables. Student t-test was also performed and yielded similar statistical significance as the Wilcoxon test. Statistical significance was set at a p value of <0.05. The relationship between myofiber tension (normalized to fiber area) and sarcomere length was modeled as a polynomial regression as previously described [13] and differences between groups compared by ANOVA.

Results

Cardiac chamber geometry and hemodynamics

Table 1 shows the plasma hormone, hemodynamic and geometrical characteristics of NL and HF dogs. Steady state data reflect values after volume expansion but differences between groups prior to volume expansion (data not shown) were similar. Plasma levels of ANP and cBNP were elevated in HF. At conscious echocardiography, HF dogs had LV and LA enlargement and reduced ejection fraction. At hemodynamic study, HF dogs had a lower ejection fraction, reduced end-systolic elastance (Ees) with larger Vo, LV enlargement (higher EDV), and higher LV diastolic and systolic and LA diastolic wall stress. Relaxation was more impaired, diastolic pressures were higher and the LV end-diastolic pressure-volume relationship curves were shifted to the right (Figure 1), with higher EDV_{20} values, consistent with the marked chamber remodeling. In the setting of this marked LV remodeling and despite elevated filling pressures, the stiffness coefficient β was lower, $\beta_{Normalized}$ tended to be lower and myocardial stiffness (κ) was lower in HF.

Myocardial structure

There was global cardiac hypertrophy with increased LA, RA and LV masses (indexed to body weight) and a trend toward increased RV mass (Table 2).

Collagen content was higher in atria than in the LV in NL and HF dogs. The collagen content in the atria and LV in HF dogs was similar to or lower than observed in NL dogs (Table 2).

In NL dogs, the relative expression of the compliant titin isoform (N2BA:N2B ratio) was greater in the atria and RV than in the LV (Table 2 and Figure 2). However, in HF dogs, these chamber differences were diminished. As compared to NL, the N2BA:N2B ratio was decreased in the HF group in the atria and RV but not in the LV.

LV endocardium versus epicardium

ANP and cBNP tissue concentration was or tended to be higher in the LV endocardium than epicardium in both the NL and HF groups (Table 3) and this transmural gradient was greatly increased in HF dogs. As compared to NL, NP levels were markedly higher in the failing endocardium but were slightly and not significantly higher in failing vs normal epicardium. Further, LV endocardial and epicardial BNP correlated with LV end-diastolic wall stress (Figure 3). Similar relationships also existed between tissue BNP and end-*systolic* wall stress (r=0.59 and p=0.04 for the endocardium; r=0.65 and p=0.02 for the epicardium).

Collagen content was similar in endo and epicardium in both NL and HF groups and was not different between groups.

The N2BA:N2B ratio was similar in epi- and endocardium in NL dogs but was lower in epicardium than endocardium in HF dogs. In the endocardium, the N2BA:N2B ratio was similar in HF and NL dogs. In the epicardium, the N2BA:N2B ratio was lower in HF as compared to NL dogs. Consistent with this, passive myofiber stiffness was increased in the epicardium of HF dogs as compared to HF endocardium or NL epi- or endocardium (Figure 4).

Discussion

Like human DCM, HF related to TRCM in the dog was associated with marked cardiac dilatation, LV and bi-atrial hypertrophy, LV systolic dysfunction, impaired LV relaxation, elevated LV filling pressures and increases in diastolic LV and LA wall stress. Unlike LV samples from humans with end-stage HF and DCM, collagen content was not increased in TRCM. While shifts to the more compliant titin isoform (N2BA) have been described in the LV in end-stage human HF, including DCM [12–14], here we observed decreases in the relative expression of the more compliant isoform (N2BA:N2B ratio) in the LV epicardium. Further, for the first time, we document even more dramatic decreases in the N2BA:N2B ratio in the RV and atria in TRCM. While decreased LV epicardial N2BA:N2B ratio in HF was associated with expected increases in epicardial myofiber passive stiffness, chamber mechanics and myocardial stiffness were driven by the marked remodeling (dilatation without fibrosis) with no increase in passive LV diastolic stiffness or myocardial stiffness calculated from the EDPVR data. Finally, using myocardial NP production as a molecular marker of stretch-regulated responses, we did not find evidence of impaired mechanotransduction as endocardial NP production was increased in HF, in relation to increases in wall stress.

Experimental TRCM

While different types of human and experimental DCM share many phenotypic characteristics, genetic, myocardial and chamber characteristics in human or experimental DCM may vary according to etiology and duration [22–25].

Previous studies in the TRCM model have reported LV dilatation and systolic dysfunction similar to that reported here [1–7]. The particular pacing protocol used in the current study is unique in the progressive nature of the tachy-pacing insult, a variation that seems to result in mild hypertrophy not seen in other studies which use a constant high pacing rate [6,7].

Assessment of myocardial and LV chamber passive diastolic properties in TRCM have been more variably described. Neumann et al. reported marked increases in LV diastolic stiffness in conscious dogs with TRCM [26]. However, several other studies in TRCM consistently describe a rightward shift without an increase (or with an actual decrease) in the steepness of the EDPVR or in myocardial or chamber diastolic stiffness parameters; findings consistent with those of the current study [3,5,27,28].

In terms of ECM changes, consistent with the current findings, several studies have documented no change [5,26,29] or slight decreases [3,4,28] in collagen depending on the method used to assess collagen and the sampling site. Spinale et al. also reported that collagen cross linking is decreased in TRCM and that type I and III collagen mRNA expression was unchanged [4]. Importantly, while not assessed here, several groups have reported loss of the collagen weave connecting myocytes to each other [3,30] with disruption of the lateral sarcomere alignment and Z line expansion [4,8,30] in TRCM. Further, myocytes isolated from TRCM hearts display marked reduction in attachment to constituents of the ECM basement membrane [4,8]. These findings suggest that TRCM may be characterized by fundamental defects in the coupling of the ECM to the sarcomere. While this defect is thought to contribute to the dilatation and systolic dysfunction in the model, it could also have implications for titin based mechano-sensing and even for the stimulus for titin isoform changes. Indeed, altered mechanical feedback between the matrix and the myocyte likely affects titin isoform composition[31].

Titin isoforms in experimental and human DCM

Insight into the significance of titin isoform changes in cardiac disease is complicated by developmental and possible age related changes, variability among species, chamber and transmural heterogeneity and marked functional alterations with titin phosphorylation status[9,10,32–34]. It is also impossible to determine whether the titin isoform changes observed inthis experiment are solely related to heart failure with increased wall stress or whether tachycardia itself is contributory. In fact, smaller species with higher heart rate have been shown to have a much lower N2BA:N2B ratio[32]. To date, all factors regulating alternative splicing and differential isoform expression remain unclear but a recent study suggests hormonal (thyroid (T_3), angiotensin) as well as mechanical factors may influence isoform changes from the fetal (more N2BA) to the adult (more N2B) phenotype through PI3K/Akt-dependent signaling[31]. In humans with advanced HF due to ischemic or non-ischemic DCM, LV samples were shown to have an *increased* cardiac N2BA:N2B ratio suggesting reversion to a fetal phenotype [12–14] as well as increases in total collagen and increases in the ratio of type I to type II collagen [35,36]. Experimental evidence suggested an inverse relationship between collagen stiffness and titin stiffness in chronic human end-stage cardiomyopathy, including DCM [12–14], as well as in myocardium of a hypothyroid rat model[37]. In the study of Nagueh et al in human DCM, decreases in relative N2BA expression correlated with worse LV diastolic function as assessed by echocardiography [12].

In dogs with TRCM (2 weeks tachy-pacing), Bell et al. [15] demonstrated a lower-than-normal N2BA:N2B ratio in the epicardium but unchanged titin-isoform composition in mid-wall segments and an increased N2BA:N2B ratio in the endocardium; the transmural gradient thus tended to be more prominent in TRCM dogs. Wu et al. [16] observed a lower N2BA:N2B ratio in the mid myocardial segment in dogs with TRCM (4 weeks tachy-pacing), a finding associated with increases in ex-vivo, mid myocardial myofiber passive stiffness. These findings are not disparate with our own. However, Wu et al. also reported that collagen-based muscle stiffness determined in KCl/KI treated myofibers was increased and speculated that increased collagen-based and titin-based stiffness contribute to increases in LV diastolic stiffness in TRCM [16]. However, neither LV diastolic properties nor ECM changes were measured.

Here we confirm the findings of Wu and Bell as we found a decrease in the N2BA/N2B ratio in the epicardium in TRCM, but extend their findings by demonstrating that this change occurred in all four cardiac chambers and indeed, more dramatically in the thinner walled chambers. More importantly, by assessing the ECM and the LV diastolic properties concomitantly with titin-isoform changes, we draw different conclusions regarding the functional implications of the titin-isoform changes observed in these three studies. First, our findings and those of several other groups suggest that LV chamber and myocardial diastolic

stiffness is not increased, indeed is decreased in TRCM in the setting of marked dilatation as noted above. Thus, as acknowledged by Wu et al [16], other remodeling changes may dissociate changes in sarcomeric passive diastolic stiffness from chamber and even global myocardial stiffness. Second, we and others (as noted above) have found no increase, if anything a trend towards decreases in ECM content and no evidence of changes in collagen character which could explain increases in collagen-based stiffness in TRCM, consistent with the findings in regard to chamber and myocardial stiffness seen here and by others as noted above.

In regards to a potential role for uncoupling of the ECM and the sarcomere in TRCM in contributing to differences in titin-based mechanical signaling in human DCM and experimental TRCM, we did not find evidence of a loss of mechanotransduction (at least in the endocardial layers) as increases in NP production in the endocardium were intact and were related to LV diastolic wall stress. Increases in NP production by the LV myocardium occur in response to wall stress and a transmural difference with greater NP in the endocardium has been reported in humans with end-stage HF due to ischemic or non-ischemic DCM [38] where total NP content, as well as the endo- to epicardial gradient decreased with unloading of the LV with a ventricular assist device. The Z-disk mechanosensor involves titin, telethonin and muscle specific LIM protein (MLP). Disruption of this complex in a MLP-null mouse model resulted in DCM. In neonatal cardiomyocytes cultured from MLP-null mice, loss of upregulation of BNP in response to stretch but not pharmacological stimulation was observed [11]. Thus, the preservation of NP activation in the endocardium in TRCM suggests that the stress-sensing function of the cardiomyocyte is intact. While NP production can also be up-regulated due to biochemical pathways, NP production correlated with wall stress and was not increased significantly in the epicardium suggesting that the up-regulation was not primarily hormonally mediated. While stress is expected to increase in both epicardial and endocardial layers in HF, there is probably an exaggerated increase in stress in the endocardium compared to the epicardium[39], leading to more prominent changes in endocardial vs epicardial NP (especially that the relationship between stress and NP production may be exponential rather than linear, as suggested by Figure 3). The NP increase in the epicardium may have been too small in this small sample size (n=6) to be statistically significant. In fact, there was a positive correlation between wall stress and both endocardial and epicardial Log (BNP).

In the absence of unique disruption of stress-sensing, the mechanism for differential changes in titin isoform expression in human DCM and experimental TRCM remains unclear as both human HF and this model are characterized by increases in wall stress, activation of the renin-angiotensin-aldosterone system [7] and alterations in thyroid function consistent with a “euthyroid sick” state [40]. As titin composition is altered via induction of the PI3K/Akt pathway during heart development[31] a possibility is that one or more of the many triggers of this pathway activate the transition towards increased N2B proportions in TRCM.

It is of note that the atria and RV showed dramatic reduction in the more compliant isoform expression. While both ventricles are subjected to tachycardia stress, ventricular-atrial conduction may not be 1:1 and the elevated ventricular filling pressures may expose the atria to a more conventional pressure overload stress. While not assessed, atrial chamber properties may be more sensitive to increases in titin-based stiffness and these changes may be important in the pathophysiology of HF, as all cardiac chambers contribute to the final homeostasis.

Limitations

Atrial and RV myofiber and chamber mechanics were not assessed nor was collagen-based myofiber stiffness. Study of other canines with other etiologies of HF may provide insight into regulation of titin-isoform changes. Tachycardia by itself, besides HF, may be contributing to the titin isoform expression changes. As RV is paced first in this model, some changes observed in the atria may also be related to retrograde activation or AV dissociation with contraction

against closed valves, and may not fully represent what happens in other HF models. However, increases in atrial afterload due to elevated ventricular diastolic pressures or contracting against a closed valve still present a similar type of stress (pressure overload) to the atria. Moreover, as heart rate may alter myocardial stiffness, it would have been interesting to define myocardial properties during tachycardia, which was not done here. Studying diastolic properties during extreme tachycardia would be challenging given the very short duration of diastole and the effect of incomplete relaxation.

Conclusions

The current study demonstrates that in contrast to human HF, dogs with TRCM develop decreases in the relative expression of the N2BA titin isoform in all cardiac chambers, that LV mechanics in this model are more driven by geometric and ECM changes than by changes in titin-based myofiber stiffness and that the difference in human DCM and canine TRCM does not appear driven by disruption of stretch-regulated responses. Further understanding of the role of titin and titin-associated proteins in regulating global cardiac structure and function will require more studies in human tissue and in alternative animal models which mimic the human condition. None the less, the unique findings in TRCM may provide an opportunity to further dissect out the factors which regulate titin-isoform changes and their impact on cardiac function in disease.

In this study, we characterized titin isoform expression and extracellular matrix (ECM) in all four cardiac chambers and the left ventricular (LV) epi- and endocardium in normal dogs and those with heart failure (HF) due to tachypacing, in addition to the functional implications at the LV myofiber and chamber level. We found that all chambers were dilated in HF but the ECM was not increased. HF dogs had markedly lower ratio of the compliant titin isoform in atria and right ventricle. In failing LV, the compliant titin isoform was decreased only in the epicardium where myofiber passive stiffness was increased. However, LV chamber mechanics were driven by the marked LV dilatation with no increase in LV diastolic stiffness. Tissue natriuretic peptide levels increased dramatically in the endocardium in relation to increases in LV wall stress, suggesting that the mechanotransduction role of titin was not impaired in HF. Further understanding of the role of titin and titin-associated proteins in regulating global cardiac structure and function will require more studies in human tissue and in alternative animal models which mimic the human condition. Nonetheless, the unique findings in tachypacing canine cardiomyopathy may provide an opportunity to further dissect out the factors which regulate titin-isoform changes and their impact on cardiac function in disease.

Acknowledgments

Grant Support: Funding for this study was provided by the National Institutes of Health (NIH HL 63281; MM Redfield) and by the German Research Foundation (Grant Li 690/7-1; WA Linke)

References

1. Shinbane JS, Wood MA, Jensen DN, Ellenbogen KA, Fitzpatrick AP, Scheinman MM. Tachycardia-induced cardiomyopathy: a review of animal models and clinical studies. Journal of the American College of Cardiology 1997;29:709–715. [PubMed: 9091514]
2. Komamura K, Vatner SF. Alterations in left ventricular systolic and diastolic function in conscious dogs with pacing-induced heart failure. Jpn Circ J 1993;57(Suppl 4):1238–40. [PubMed: 7966954]
3. Spinale FG, Tomita M, Zellner JL, Cook JC, Crawford FA, Zile MR. Collagen remodeling and changes in LV function during development and recovery from supraventricular tachycardia. Am J Physiol 1991;261:H308–18. [PubMed: 1877659]

4. Spinale FG, Zellner JL, Johnson WS, Eble DM, Munyer PD. Cellular and extracellular remodeling with the development and recovery from tachycardia-induced cardiomyopathy: changes in fibrillar collagen, myocyte adhesion capacity and proteoglycans. Journal of Molecular and Cellular Cardiology 1996;28:1591–1608. [PubMed: 8877770]
5. Komamura K, Shannon RP, Pasipoularides A, Ihara T, Lader AS, Patrick TA, Gishop SP, Vatner SF. Alterations in left ventricular diastolic function in conscious dogs with pacing-induced heart failure. Journal of Clinical Investigation 1992;89:1825–1838. [PubMed: 1601992]
6. Yamamoto K, Burnett JC Jr. Meyer LM, Sinclair L, Stevens TL, Redfield MM. Ventricular remodeling during development and recovery from modified tachycardia-induced cardiomyopathy model. Am J Physiol 1996;271:R1529–34. [PubMed: 8997349]
7. Stevens, TL.; Borgeson, DD.; Luchner, A.; Wennberg, PW.; Redfield, MM.; Burnett, J. Pathophysiology of Tachycardia-Induced Heart Failure. Futura Publishing Company, Inc.; New York, New York: 1996. J. C. A modified model of tachycardia-induced cardiomyopathy: Insights into humoral and renal adaptations.
8. Zellner JL, Spinale FG, Eble DM, Hewett KW, Crawford FA Jr. Alterations in myocyte shape and basement membrane attachment with tachycardia-induced heart failure. Circ Res 1991;69:590–600. [PubMed: 1873861]
9. Linke WA. Sense and stretchability: the role of titin and titin-associated proteins in myocardioal stress-sensing and mechanical dysfunction. Cardiovasc Res. Apr 6;2007 epub ahead of print
10. LeWinter MM, Wu Y, Labeit S, Granzier H. Cardiac titin: structure, functions and role in disease. Clin Chim Acta 2007;375:1–9. [PubMed: 16904093]
11. Knoll R, Hoshijima M, Hoffman HM, Person V, Lorenzen-Schmidt I, Bang ML, Hayashi T, Shiga N, Yasukawa H, Schaper W, McKenna W, Yokoyama M, Schork NJ, Omens JH, McCulloch AD, Kimura A, Gregorio CC, Poller W, Schaper J, Schultheiss HP, Chien KR. The cardiac mechanical stretch sensor machinery involves a Z disc complex that is defective in a subset of human dilated cardiomyopathy. Cell 2002;111:943–55. [PubMed: 12507422]
12. Nagueh SF, Shah G, Wu Y, Torre-Amione G, King NM, Lahmers S, Witt CC, Becker K, Labeit S, Granzier HL. Altered titin expression, myocardial stiffness, and left ventricular function in patients with dilated cardiomyopathy. Circulation 2004;110:155–62. [PubMed: 15238456]
13. Makarenko I, Opitz CA, Leake MC, Neagoe C, Kulke M, Gwathmey JK, del Monte F, Hajjar RJ, Linke WA. Passive stiffness changes caused by upregulation of compliant titin isoforms in human dilated cardiomyopathy hearts. Circ Res 2004;95:708–16. [PubMed: 15345656]
14. Neagoe C, Kulke M, del Monte F, Gwathmey JK, de Tombe PP, Hajjar RJ, Linke WA. Titin isoform switch in ischemic human heart disease. Circulation 2002;106:1333–41. [PubMed: 12221049]
15. Bell SP, Nyland L, Tischler MD, McNabb M, Granzier H, LeWinter MM. Alterations in the determinants of diastolic suction during pacing tachycardia. Circ Res 2000;87:235–40. [PubMed: 10926875]
16. Wu Y, Bell SP, Trombitas K, Witt CC, Labeit S, LeWinter MM, Granzier H. Changes in titin isoform expression in pacing-induced cardiac failure give rise to increased passive muscle stiffness. Circulation 2002;106:1384–9. [PubMed: 12221057]
17. Maniu CV, Patel JB, Reuter DG, Meyer DM, Edwards WD, Rihal CS, Redfield MM. Acute and chronic reduction of functional mitral regurgitation in experimental heart failure by percutaneous mitral annuloplasty. J Am Coll Cardiol 2004;44:1652–61. [PubMed: 15489099]
18. Burkhoff D, Mirsky I, Suga H. Assessment of systolic and diastolic ventricular properties via pressure-volume analysis: a guide for clinical, translational, and basic researchers. Am J Physiol Heart Circ Physiol 2005;289:H501–12. [PubMed: 16014610]
19. Hart CY, Meyer DM, Tazelaar HD, Grande JP, Burnett JC Jr. Housmans PR, Redfield MM. Load versus humoral activation in the genesis of early hypertensive heart disease. Circulation 2001;104:215–220. [PubMed: 11447089]
20. Munagala VK, Hart CY, Burnett JC Jr. Meyer DM, Redfield MM. Ventricular structure and function in aged dogs with renal hypertension: a model of experimental diastolic heart failure. Circulation 2005;111:1128–35. [PubMed: 15723971]

21. Shapiro BP, Lam CS, Patel JB, Mohammed SF, Kruger M, Meyer DM, Linke WA, Redfield MM. Acute and chronic ventricular-arterial coupling in systole and diastole: insights from an elderly hypertensive model. Hypertension 2007;50:503–11. [PubMed: 17620524]
22. Yarbrough WM, Mukherjee R, Brinsa TA, Dowdy KB, Scott AA, Escobar GP, Joffs C, Lucas DG, Crawford FA Jr. Spinale FG. Matrix metalloproteinase inhibition modifies left ventricular remodeling after myocardial infarction in pigs. J Thorac Cardiovasc Surg 2003;125:602–10. [PubMed: 12658202]
23. Zile MR, Tomita M, Nakano K, Mirsky I, Usher B, Lindroth J, Carabello BA. Effects of left ventricular volume overload produced by mitral regurgitation on diastolic function. Am J Physiol 1991;261:H1471–80. [PubMed: 1951734]
24. Gaasch WH, Cole JS, Quinones MA, Alexander JK. Dynamic determinants of letf ventricular diastolic pressure-volume relations in man. Circulation 1975;51:317–23. [PubMed: 122921]
25. Williams RE, Kass DA, Kawagoe Y, Pak P, Tunin RS, Shah R, Hwang A, Feldman AM. Endomyocardial gene expression during development of pacing tachycardia-induced heart failure in the dog. Circ Res 1994;75:615–23. [PubMed: 7923607]
26. Neumann T, Vollmer A, Schaffner T, Hess OM, Heusch G. Diastolic dysfunction and collagen structure in canine pacing-induced heart failure. J Mol Cell Cardiol 1999;31:179–92. [PubMed: 10072726]
27. Solomon SB, Nikolic SD, Glantz SA, Yellin EL. Left ventricular diastolic function of remodeled myocardium in dogs with pacing-induced heart failure. Am J Physiol 1998;274:H945–54. [PubMed: 9530208]
28. Spinale FG, Coker ML, Krombach SR, Mukherjee R, Hallak H, Houck WV, Clair MJ, Kribbs SB, Johnson LL, Peterson JT, Zile MR. Matrix metalloproteinase inhibition during the development of congestive heart failure : effects on left ventricular dimensions and function. Circ Res 1999;85:364–76. [PubMed: 10455065]
29. Wilson JR, Douglas P, Hickey WF, Lanoce V, Ferraro N, Muhammad A, Reichek N. Experimental congestive heart failure produced by rapid ventricular pacing in the dog: cardiac effects. Circulation 1987;75:857–67. [PubMed: 3829344]
30. Komamura K, Shannon RP, Ihara T, Shen YT, Mirsky I, Bishop SP, Vatner SF. Exhaustion of Frank-Starling mechanism in conscious dogs with heart failure. Am J Physiol 1993;265:H1119–31. [PubMed: 8238398]
31. Kruger M, Sachse C, Zimmermann WH, Eschenhagen T, Klede S, Linke WA. Thyroid hormone regulates developmental titin isoform transitions via the PI3K/AKT pathway. Circ Res Dec 20;2007epub ahead of print
32. Cazorla O, Freiburg A, Helmes M, Centner T, McNabb M, Wu Y, Trombitas K, Labeit S, Granzier H. Differential expression of cardiac titin isoforms and modulation of cellular stiffness. Circ Res 2000;86:59–67. [PubMed: 10625306]
33. Wu Y, Cazorla O, Labeit D, Labeit S, Granzier H. Changes in titin and collagen underlie diastolic stiffness diversity of cardiac muscle. J Mol Cell Cardiol 2000;32:2151–62. [PubMed: 11112991]
34. Kruger M, Kohl T, Linke WA. Developmental changes in passive stiffness and myofilament Ca2+ sensitivity due to titin and troponin-I isoform switching are not critically triggered by birth. Am J Physiol Heart Circ Physiol 2006;291:H496–506. [PubMed: 16679402]
35. Marijianowski MM, Teeling P, Mann J, Becker AE. Dilated cardiomyopathy is associated with an increase in the type I/type III collagen ratio: a quantitative assessment. J Am Coll Cardiol 1995;25:1263–72. [PubMed: 7722119]
36. Gunja-Smith Z, Morales AR, Romanelli R, Woessner JF Jr. Remodeling of human myocardial collagen in idiopathic dilated cardiomyopathy. Role of metalloproteinases and pyridinoline cross-links. Am J Pathol 1996;148:1639–48. [PubMed: 8623931]
37. Wu Y, Peng J, Campbell KB, Labeit S, Granzier H. Hypothyroidism leads to increased collagen-based stiffness and re-expression of large cardiac titin isoforms with high compliance. J Mol Cell Cardiol 2007;42:186–95. [PubMed: 17069849]
38. Altemose GT, Gritsus V, Jeevanandam V, Goldman B, Margulies KB. Altered myocardial phenotype after mechanical support in human beings with advanced cardiomyopathy. J Heart Lung Transplant 1997;16:765–73. [PubMed: 9257259]

39. Yin FC. Ventricular wall stress. Circ Res 1981;49:829–42. [PubMed: 7023741]
40. Panciera DL, Refsal KR. Thyroid function in dogs with spontaneous and induced congestive heart failure. Can J Vet Res 1994;58:157–62. [PubMed: 7954115]

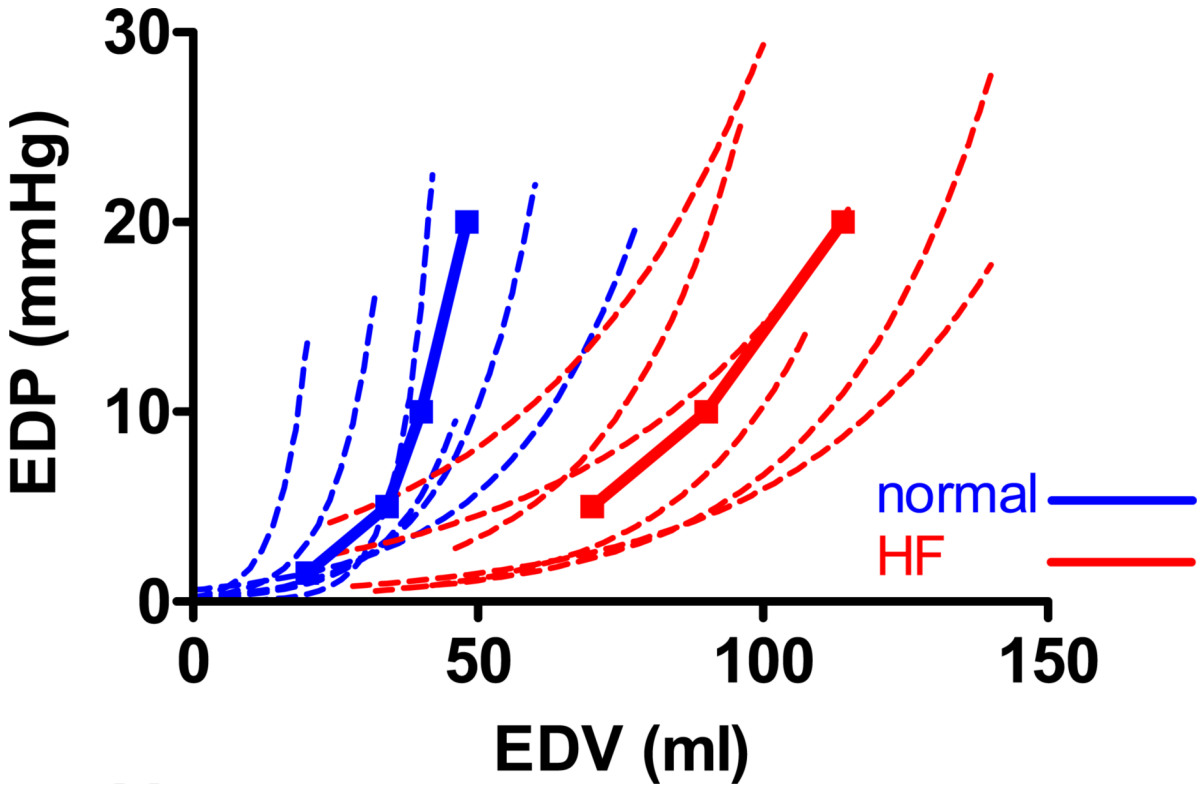

Figure 1.
Individual end diastolic passive pressure-volume relationships (dashed lines) of all normal (normal, blue) and heart failure (HF, red) dogs defined during acute caval occlusion with the average curve (solid lines) for each group. Compared to the normal group, HF dogs have the diastolic stiffness curve shifted to the right, with a modest decrease in the slope.

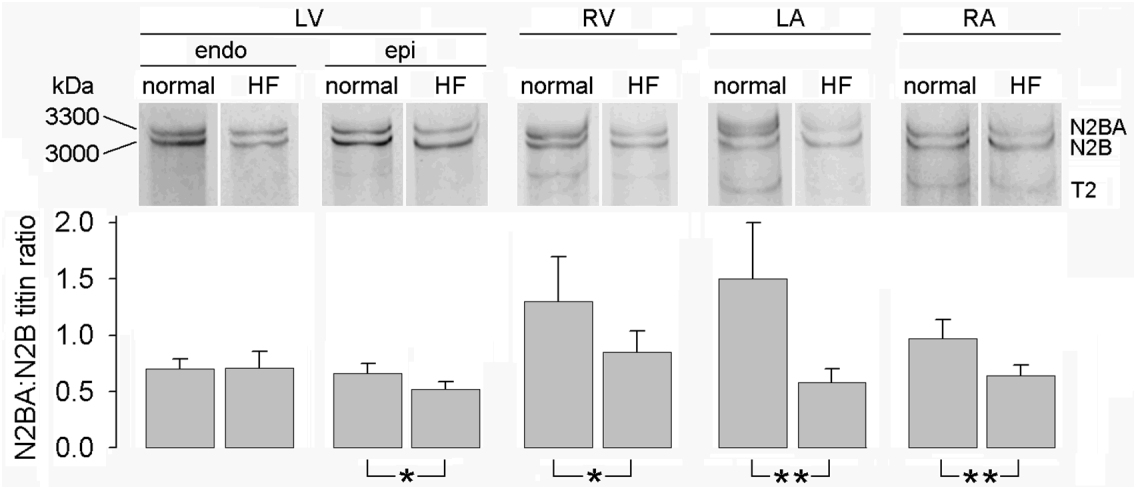

Figure 2.

Representative gels and summary of data showing relative content of N2B and N2BA titin isoforms in left ventricle (LV) endocardium (endo) and epicardium (epi), right ventricle (RV) and left (LA) and right (RA) atrial tissue from normal and heart failure (HF) dogs.

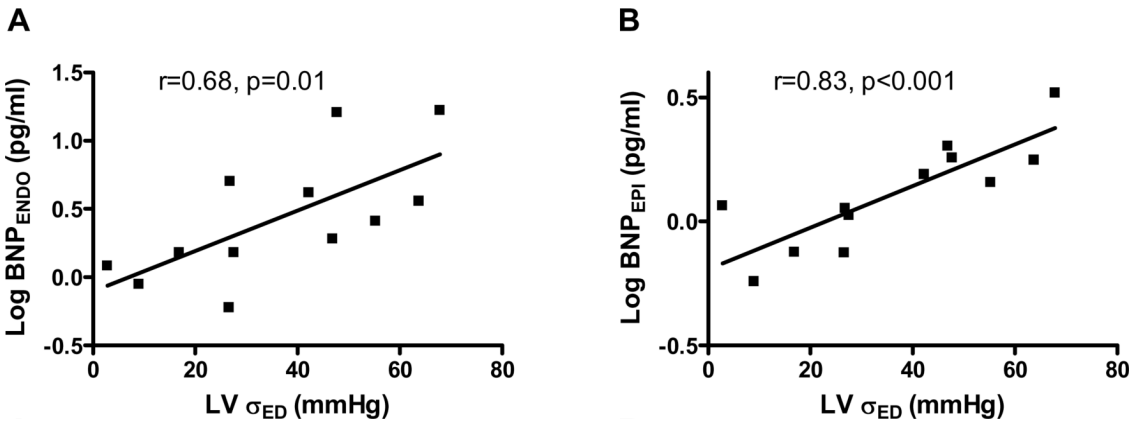

Figure 3.
LV endocardial (A) and epicardial (B) BNP concentration (log transformed) increases with increases in LV end diastolic wall stress (LVσED) in normal and HF dogs.

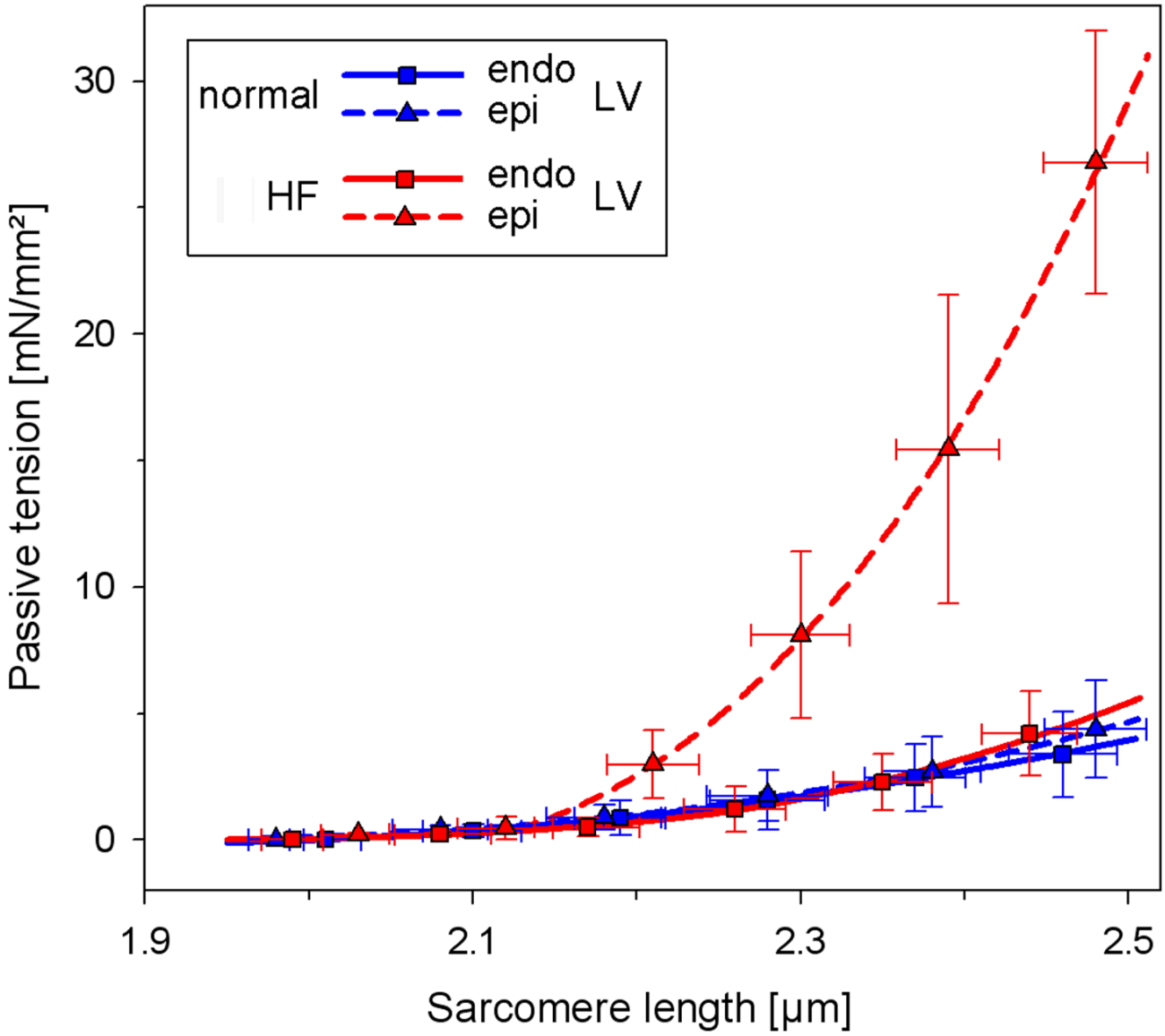

Figure 4.
Passive myofiber stiffness curves in left ventricle (LV) endocardium (endo) and epicardium (epi) from normal and heart failure (HF) dogs. Stiffness is increased in the HF epicardium as compared to HF endocardium and normal epicardium or endocardium ($p<0.05$ for all). Bars are standard deviations.

Table 1

Cardiac geometry and hemodynamic variables

	Normal (NL, n=6)	Heart Failure (HF, n=6)	p HF vs NL
Plasma hormones			
Plasma ANP (pg/ml)	58 ± 48	257 ± 137	0.01
Plasma cBNP (pg/ml)	11 ± 1	68 ± 42	0.006
Conscious echocardiography			
LV end diastolic dimension (cm)	4.06 ± 0.31	4.96 ± 0.19	0.0002
Ejection Fraction (%)	62 ± 6	16 ± 8	0.0001
Left atrial volume (ml)	26 ± 12	87 ± 36	0.006
Hemodynamic study			
Systolic function			
Heart rate (bpm)	108 ± 13	107 ±15	0.9
LV peak systolic pressure (mmHg)	104 ± 10	94 ± 23	0.3
Ejection Fraction (%)	53 ± 8	26 ± 4	0.0001
End systolic elastance (Ees, mmHg/ml)	11.5 ± 9.0	2.1 ± 0.8	0.008
V_0 (ml)	6.3 ± 8.6	27.7 ± 15.2	0.01
Diastolic function			
LV end diastolic volume (ml)	46.5 ± 21.4	110 ± 20	0.004
LV end diastolic pressure (mmHg)	15 ± 7	25 ± 6	0.02
tau (ms)	36 ± 12	82 ± 31	0.01
LV diastolic stiffness coefficent (β, mmHg/ml)	0.13 ± 0.06	0.03 ± 0.01	0.004
α	0.21 ± 0.20	0.89 ± 0.93	0.3
$\beta_{Normalized}$ (mmHg)	10.53 ± 4.16	3.86 ± 1.07	0.02
Myocardial stiffness index (κ)	12.50 ± 3.56	8.45 ± 1.93	0.04
LV capacitance (EDV_{20}, ml)	46 ± 19	112 ± 29	0.004
Wall stress			
LV end systolic wall stress (σES, mmHg)	64 ± 27	131 ± 55	0.01
LV end diastolic wall stress (σED, mmHg)	21 ± 16	50 ± 15	0.02
Left atrial diastolic wall stress (σED, mmHg)*	47 ± 44	124 ± 44	0.02

Abbreviations: ANP, atrial natriuretic peptide; cBNP, canine brain natriuretic peptide; LV, left ventricular

* pre-volume expansion

Table 2

Cardiac chamber hypertrophy, ECM and titin isoform profile

	Normal (NL, n=6)	Heart Failure (HF, n=6)	p HF vs NL
Cardiac chamber hypertrophy			
LA weight/body weight (g/Kg)	0.40±0.11	1.03±0.16	<0.0001
RA weight/body weight (g/Kg)	0.27±0.04	0.72±0.13	<0.0001
RV weight/body weight (g/Kg)	1.38±0.28	1.54±0.08	0.3
LV weight/body weight (g/Kg)	4.07±0.61	5.22±0.61	0.01
Cardiac chamber collagen			
LA collagen (μg/mg tissue)	12.9 ± 6.3*	10.9 ± 0.6*	0.6
RA collagen (μg/mg tissue)	18.5 ± 4.1*	12.7 ± 2.3*	0.02
LV collagen (μg/mg tissue)	5.0 ± 1.6	4.9 ± 0.6	0.6
Cardiac chamber N2BA:N2B expression			
LA N2BA:N2B ratio	1.5±0.5*	0.58±0.12	0.003
RA N2BA:N2B ratio	0.97±0.17*	0.64±0.1	0.01
RV N2BA:N2B ratio	1.30±0.4*	0.85±0.2	0.04
LV N2BA:N2B ratio	0.68 ± 0.10	0.63 ± 0.13	0.4

Abbreviations: LA, left atrial; RA, right atrial; RV, right ventricular; LV, left ventricular

* $p < 0.05$ vs LV

Table 3

Natriuretic peptide concentration, collagen content, and titin isoform expression in the left ventricular epicardium vs endocardium.

	Normal (NL, n=6)	Heart Failure (HF, n=6)	p HF vs NL
ANP (pg/mg protein)			
epicardial	1.7 ± 0.4	4.0 ± 5.5	0.8
endocardial	7.8 ± 5.2*	23 ± 9*	0.01
cBNP (pg/ mg protein)			
epicardial	1.0 ± 0.5	1.5 ± 0.3	0.06
endocardial	1.3 ± 0.5	8.0 ± 6.5*	0.004
Collagen (µg/mg tissue)			
epicardial	5.5 ± 0.8	5.3 ± 0.9	0.7
endocardial	5.0 ± 1.6	4.5 ± 0.6	0.5
Collagen volume fraction (%)			
epicardial	2.21 ± 0.92	1.99 ± 1.17	0.8
endocardial	1.27 ± 0.74	1.79 ± 1.43	0.4
Titin N2BA:N2B ratio			
epicardial	0.66 ± 0.09	0.52 ± 0.07	0.03
endocardial	0.70 ± 0.09	0.71 ± 0.15*	0.8

Abbreviations: ANP, atrial natriuretic peptide; cBNP, canine brain natriuretic peptide; LV, left ventricular

* $p < 0.05$ vs epicardial